Ab Initio Molecular Dynamics Simulations of Ionic Liquids

Jindal K. Shah[1]
School of Chemical Engineering, Oklahoma State University, Stillwater, OK, United States
[1] Corresponding author: *Email address:* jindal.shah@okstate.edu (J.K. Shah)

Contents

Abstract

Room temperature ionic liquids are solvents comprised of molecular cations and anions. The negligible vapor pressure of these solvents coupled with the ability to design an ionic liquid by forming different combinations of cations and anions has been the main drivers for the attention they are receiving in academia and industry alike. Given the large number of possible ionic liquids, molecular simulation and computational chemistry-based methods have been applied to calculate electronic, thermophysical, and phase-equilibria properties of ionic liquids. In this chapter, our focus is on the ab initio molecular dynamics simulations to demonstrate ionic liquid phenom-

Annual Reports in Computational Chemistry, Volume xx
ISSN 1574-1400, https://doi.org/10.1016/bs.arcc.2018.08.001

ena that are difficult to capture with force field-based approaches by providing several examples.

1. INTRODUCTION

Room temperature ionic liquids are defined as solvents that are composed of molecular cations and anions. The cation is usually or-

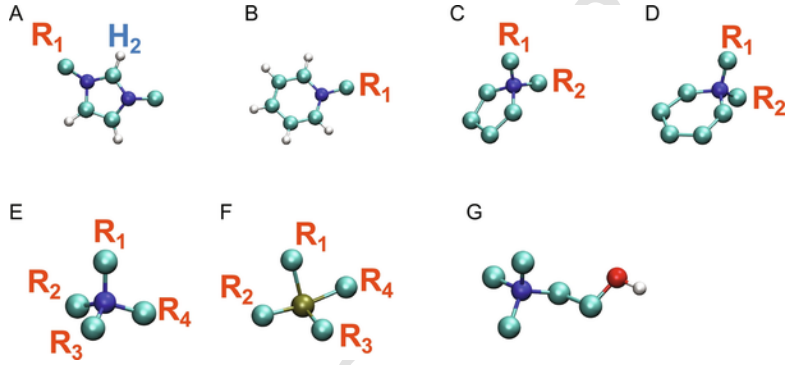

Fig. 1. Representative cations classes forming ionic liquids: (A) 1-alkyl-3-methylimidazolium, (B) 1-alkylpyridinium, (C) *N*,*N*-dialkylpyrrolidinium, (D) *N*,*N*-dialkylpiperidinium, (E) tetraalkylammonium, (F) tetraalkylphosphonium, (G) cholinium. The most acidic proton in the imidazolium ionic liquid is identified as H_2. Hydrogen atoms bonded to carbon atoms are not shown for clarity in (C), (D), and (G). A large number of cations can be envisioned by changing the identity of the pendant groups R_1, R_2, R_3, and R_4. Color coding: carbon—*cyan*, nitrogen—*blue*, hydrogen—*white*, phosphorus—*tan*, oxygen—*red*.

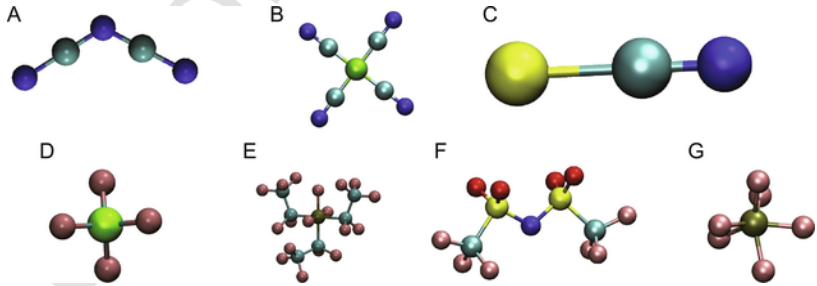

Fig. 2. Representative anions forming ionic liquids: (A) dicyanamide $[N(CN)_2]^-$, (B) tetracyanoborate $[B(CN)_4]^-$, (C) thiocyanate $[SCN]^-$, (D) tetrafluoroborate $[BF_4]^-$, (E) tris(pentafluoroethyl)trifluorophosphate, (F) bis(trifluoromethanesulfonyl)imide $[NTf_2]^-$, (G) hexafluorophosphate $[PF_6]^-$. Color coding: carbon—*cyan*, nitrogen—*blue*, boron—*green*, sulfur—*yellow*, fluorine—*pink*, oxygen—*red*, phosphorus—*tan*.

TABLE 1 Representative Sampling of Ionic Liquids Along With Details on AIMD Simulations

Cation	Anion	#	Theory	Basis Set	Pseudopotential	Simulation Time (ps)	Package
[C_1mim]	Oxalatoborate	56	BLYP-D3	MOLOPT-DZVP-SR-GTH	GTH	48	CP2K [81]
[Ch]	Valine	12	PBE-D3	MOLOPT-DZVP-SR-GTH	GTH	40	CP2K
[Ch]	Valine	3	PBE-D3	MOLOPT-DZVP-SR-GTH	GTH	36	CP2K
[Ch]	Norvaline	12	PBE-D3	MOLOPT-DZVP-SR-GTH	GTH	60	CP2K
[Ch]	Noraline	3	PBE-D3	MOLOPT-DZVP-SR-GTH	GTH	45	CP2K
[Ch]	Leucine	12	PBE-D3	MOLOPT-DZVP-SR-GTH	GTH	36	CP2K
[Ch]	Leucine	3	PBE-D3	MOLOPT-DZVP-SR-GTH	GTH	45	CP2K
[Ch]	Norleucine	12	PBE-D3	MOLOPT-DZVP-SR-GTH	GTH	60	CP2K
[Ch]	Norleucine	3	PBE-D3	MOLOPT-DZVP-SR-GTH	GTH	48	CP2K

TABLE 1 (Continued)

Cation	Anion	#	Theory	Basis Set	Pseudopotential	Simulation Time (ps)	Package
[Ch]	Alaninate	12	PBE-D3	MOLOPT-DZVP-SR-GTH	GTH	56	CP2K [84]
[Ch]	Alaninate	55	PBE-D3	MOLOPT-DZVP-SR-GTH	GTH	30	CP2K
[Ch]	Prolinate	15	PBE-D3	MOLOPT-DZVP-SR-GTH	GTH	56.3	CP2K
[Ch]	Prolinate	50	PBE-D3	MOLOPT-DZVP-SR-GTH	GTH	47	CP2K
[Ch]	Phenylalanine	10	PBE-D3	MOLOPT-DZVP-SR-GTH	GTH	85.6	CP2K
[Ch]	Phenylalanine	45	PBE-D3	MOLOPT-DZVP-SR-GTH	GTH	32	CP2K
[Ch]	Cysteine	12	PBE-D3	MOLOPT-DZVP-SR-GTH	GTH	79.5	CP2K
[Ch]	Histidine	15	PBE-D3	MOLOPT-DZVP-SR-GTH	GTH	53.1	CP2K
[Ch]	Cysteinate	56	PBE-D3	MOLOPT-DZVP-SR-GTH	GTH	24.4	CP2K

TABLE 1 (Continued)

Cation	Anion	#	Theory	Basis Set	Pseudopotential	Simulation Time (ps)	Package
[Ch]	Threoninate	50	PBE-D3	MOLOPT-DZVP-SR-GTH	GTH	12.8	CP2K
[Ch]	Formate	12	PBE	Plane wave (70 Ry)	DCACP	13	CPMD [86]
[Ch]	Propionate	10	PBE	Plane wave (70 Ry)	DCACP	13	CPMD
[Ch]	Butanoate	9	PBE	Plane wave (70 Ry)	DCACP	13	CPMD
Propylammonium	Nitrate	32	PBE-D3	MOLOPT-DZVP-SR-GTH	GTH	40	CP2K [87]
[C_2mim]	Acetate	1	BLYP-D2	MOLOPT-DZVP-SR-GTH	GTH	98.1	CP2K [82]
[C_2mim]	Acetate	3	BLYP-D2	MOLOPT-DZVP-SR-GTH	GTH	144.6	CP2K
[C_2mim]	Acetate	6	BLYP-D2	MOLOPT-DZVP-SR-GTH	GTH	261.0	CP2K
[C_2mim]	Acetate	12	BLYP-D2	MOLOPT-DZVP-SR-GTH	GTH	266.3	CP2K
[C_2mim]	Acetate	16	BLYP-D2	MOLOPT-DZVP-SR-GTH	GTH	170.2	CP2K

ganic in nature (Fig. 1), while the anion can be both organic or inorganic (Fig. 2). The low charge density and articulated structures of the constituent ions resist crystallization at room temperature. Ionic liquids have been known for a long time. For example, ethanolammonium nitrate (melting point 52–55°C) was reported in 1888 [1]. An early report of a room temperature ionic liquid, ethylammonium nitrate (melting point 12°C), was reported in 1914 [2]. More recently, ionic liquids were developed as potential electrolytes in the 1970s and 1980s [3–5]. Since the discovery of air- and water-stable ionic liquids in 1992 [6], ionic liquids have transitioned from academic curiosity to industrial-scale applications such as Chevron's ISOALKY process for alkylation [7], mercury removal from natural gas by Petronas [8], and gas chromatography columns [9]. The continued interest in the field of ionic liquids stems from the fact that many ionic liquids can be designed to be essentially nonvolatile. Additionally, the availability of a large number of cations and anions coupled with practically limitless opportunities of combining two ionic liquids [10–12] affords flexibility in selecting ionic liquids to meet requirements for a given process. It is no surprise that ionic liquids have been dubbed as “designer” or “task-specific” solvents. As a given ionic liquid contains both polar and nonpolar components in the cation–anion architecture, they are ideal candidates for solvating both polar and nonpolar substances. Many ionic liquids also possess a wide electrochemical window making them suitable as electrolytes. These fascinating properties of ionic liquids have enabled their applications in diverse fields such as gas separation [13–16], dye-sensitized solar cells [17–19], reaction media [20, 21], battery electrolytes [22–24], electroplating [25, 26], and chromatography [27, 28] to name a few.

According to one estimate, as many as one million ionic liquids could be formed from available cation–anion combinations [29]. Although this is attractive from the design standpoint, identifying a suitable ionic liquid to meet the specification for a given process is a daunting task as synthesizing a large number of ionic liquids and measuring relevant properties experimentally is extremely time-consuming and challenging, if not impossible. Recognizing this difficulty, molecular simulation-based approaches that take into account the knowledge of interaction between various moieties in ionic liquids have been applied since the very beginning of modern ionic liquid research. These simula-

tion methodologies can be broadly classified into three categories: (a) classical simulations; (b) electronic structure calculations; and (c) ab initio simulations. In the following, we provide a brief description of classical and ab initio molecular dynamics (AIMD) simulations followed by representative examples of AIMD simulation of ionic liquids.

2. CLASSICAL SIMULATIONS

2.1. Force Field

Classical simulation methodology relies on describing the interaction between atomic sites by a potential function termed as force field. An example of a force field functional form is given in Eq. (1).

$$E_{\text{tot}} = \sum_{\text{bonds}} K_r (r - r_0)^2 + \sum_{\text{angles}} K_\theta (\theta - \theta_0)^2 + \sum_{\text{dihedrals}} K_\chi [1 + \cos(n\chi - \delta_\chi)] + \sum_{\text{improper}} K_\psi [1 + \cos(n\psi - \\ + \sum_{i=1}^{N-1} \sum_{i<j}^{N} \left\{ 4\epsilon_{ij} \left[\left(\frac{\sigma_{ij}}{r_{ij}} \right)^{12} - \left(\frac{\sigma_{ij}}{r_{ij}} \right)^{6} \right] + \left(\frac{q_i q_j}{r_{ij}} \right) \right\}$$

The functional form suggests that the total energy of the system E_{tot} is composed of intramolecular and intermolecular interactions. The intramolecular energetic contributions include bond stretching, angle bending, dihedral angle rotations, and improper torsion for the first four sums, respectively. The terms K_r, K_θ, K_χ, K_ψ represent the respective force constants. The intramolecular and intermolecular nonbonded interactions are described by the Lennard-Jones (LJ) 12-6 potential, while the electrostatic energy is handled via Coulomb's law; σ_{ij} and ϵ_{ij} are the energy and size parameters between atoms i and j for the LJ interactions, and q_i denotes the charge on atom i. An entire set of such parameters for different ionic liquids have been proposed [30–42] and validated by predicting thermophysical and phase-equilibria properties and comparing such predictions with experimental measurements.

2.2. Simulation Methodology

Once the force field for a given ionic liquid is selected, two main molecular simulation techniques are available for ionic liquid property computation: Monte Carlo and molecular dynamics. The choice of a simulation methodology is dictated by the properties of interest. In a molec-

ular dynamics (MD) simulation, Newton's equations of motion are integrated to generate the position and velocities of ionic liquid cations and anions. Thus, MD is deterministic in nature and ideally suited for the computation of thermodynamic properties such as density, isothermal compressibility, and volume expansivity and transport properties such as self-diffusion coefficients, viscosity, and thermal conductivity. Several open-source packages such as LAMMPS [43], Gromacs [44], NAMD [45], and DL_POLY [46] are available to the research community for performing such calculations.

Monte Carlo (MC) simulation technique, on the other hand, is stochastic in nature and is designed to sample microstates (defined by the relative positions of ionic liquid cations and anions) conforming to a given ensemble probability distribution. During a MC simulation, moves that produce different microstates are attempted with a fixed probability; the acceptance of these moves is conditional upon the Metropolis criterion [47]. Examples of such moves include translation and rotation of a molecule, increase or decrease of the system volume, and insertion or deletion of a molecule to achieve chemical equilibrium. MC simulations can be employed to calculate thermodynamic properties of ionic liquids. As no time-dependent information can be obtained from a MC simulation, transport properties cannot be predicted with MC. However, the power of MC simulation lies in its ability to predict phase-equilibria properties of ionic liquids, which are extremely challenging using MD simulations due to the long times needed to reach equilibrium. Given the specialized nature of the MC moves and considerable freedom available to develop such moves, very few open-source Monte Carlo packages currently exist. We recommend Cassandra [48] and Towhee [49] for performing ionic liquid simulations.

2.3. Molecular Models

In addition to the selection of a simulation approach and force field, a decision also needs to be made regarding the molecular-level details necessary for accurate predictions of properties of interest. Several choices are available: (a) all-atom (AA) model; (b) united-atom (UA) model; and (c) coarse grain (CG) model. In an AA model, all the atomic sites are explicitly included during the course of a simulation providing a faithful molecular-level representation of the system at hand, albeit at a high computational cost. As opposed to this, a UA rep-

resentation of ionic liquid cations and anions usually implies that hydrogen atoms and the heavy atom to which they are bonded are treated as a single interaction site. In some instances, a spherical anion such as hexafluorophosphate $[PF_6]^-$ is also modeled as one site [30]. The reduction in the number of atoms results in considerable decrease in the computational time required for a given simulation as the computational cost increases roughly as the square of the number of particles in a system. Given the computational power available today, this is less of a concern. The united-atom models, however, are extremely useful in MC simulations, especially for phase-equilibria calculations as the number of degrees of freedom that need to be sampled during a MC simulation is drastically reduced. Molecular models that combine two or more groups such as methylene units into one interaction unit have also been developed. The so-called coarse-grained (CG) models enable access to phenomena occurring at long length scales and/or time scales [50–52].

2.4. Inclusion of Polarization

In many ionic liquid simulations, the partial charges on atomic sites are held fixed and as such they do not respond to the changing ionic environment around them. Although such fixed charge force fields perform well for the prediction of thermodynamic quantities, the transport properties calculated using fixed charge models have generally been found to be lower than the corresponding experimental values. The absence of explicit treatment of polarization in fixed charge models has been shown to contribute to the slower ionic liquid dynamics. One strategy to account for induced polarization is to scale the cation and anion unit charges based on the observation that the gas phase electronic structure calculations of a cation–anion pair results in the overall charge on the ions that is less than unity. Scaling factors ranging from 0.7 to 0.9 have been applied in the literature with 0.8 being the most common [37–39, 53]. The lowering of the overall charge on the cation and anion has been demonstrated to yield faster dynamics and an improvement in the agreement between simulation results and experimental measurement.

Explicit treatment of polarization requires inclusion of atomic polarizabilities in the force field functional form given in Eq. (1). The modified force field then takes the form of Eq. (2) [54, 55]

$$E_{\text{tot}} = \sum_{\text{bonds}} K_r(r - r_0)^2 + \sum_{\text{angles}} K_\theta(\theta - \theta_0)^2 + \sum_{\text{dihedrals}} K_\chi[1 + \cos(n\chi - \delta_\chi)] + \sum_{\text{improper}} K_\psi[1 + \cos(n\psi - \\ + \sum_{i=1}^{N-1} \sum_{i<j}^{N} \left\{ 4\epsilon_{ij} \left[\left(\frac{\sigma_{ij}}{r_{ij}} \right)^{12} - \left(\frac{\sigma_{ij}}{r_{ij}} \right)^{6} \right] + \left(\frac{q_i q_j}{r_{ij}} \right) \right\} - \frac{1}{2} \sum_i \vec{\mu}$$

where the induced dipole $\vec{\mu}_i$ is calculated as the product of the isotropic atomic polarizability α_i and the total electrostatic field ($\vec{E}^{\text{tot}}$) generated at the site *i* due to the fixed charges as well as induced dipole while $\vec{E}^0$ is the electric field arising from the fixed charges only. Simulations performed using Eq. (2) are computationally more demanding than the fixed charge models as a self-consistent procedure is needed to converge the induced dipole at each of the atomic sites.

The electronic polarizability has also been handled using the concept of the Drude oscillator [56, 57]. In this model, atomic sites are represented as a core and shell model. The core carries the bulk of the partial charge while the remaining charge is placed on the shell particle tethered to the core via a harmonic spring. The core–shell particle then resembles a dipole for each of the polarizable atoms and can respond to the changing ionic environment surrounding the polarizable atoms.

3. AB INITIO MOLECULAR DYNAMICS SIMULATIONS

3.1. Theory

One of the main drawbacks of the classical simulation methodologies as applied to ionic liquids is that interactions such as polarization, charge transfer, hydrogen bonding, and chemical reactions that require explicit treatment of electrons cannot be handled. Additionally, one of the fascinating aspects of the ionic liquids research is the ability to design ionic liquids in silico. In order to accurately represent various interactions in an ionic liquid, estimation of the force field parameters is required, which in turn necessitates experimental data that may not be available for such novel systems. AIMD simulation methods can circumvent such issues related to the availability of parameters due to the explicit quantum mechanical treatment of electrons. Furthermore, the ability to propagate the system via molecular dynamics method can

yield information as a function of time at quantum mechanical level. Such an approach was pioneered by Car and Parrinello in their landmark paper describing the unification of ab initio method and molecular dynamics method. In this formalism, parameters describing electronic wavefunctions are introduced as classical degrees of freedom in the equations of motion. These degrees of freedom are then propagated along with the nuclei positions obviating the need for solving electronic wavefunction at each time step [58]. As with traditional extended-system molecular dynamics approaches, fictitious masses are required while performing a Car–Parrinello molecular dynamics (CPMD) simulation.

AIMD can also be carried out in the density functional theory (DFT) framework. In this approach, the electronic density is obtained for a given set of nuclear positions by solving the Kohn–Sham orbitals and the first derivatives of the energy are obtained to get the forces. The nuclear positions and velocities are then advanced based on classical equations of motion using the calculated forces. Based on the studies referenced in this chapter, trajectories can be integrated with a larger time step in the DFT-based AIMD than that in CPMD. Irrespective of the type of approach chosen for solving the equations of motion, the inclusion of electronic degrees of freedom renders these calculations computationally demanding placing restrictions on the system size and time scales attainable in such simulations.

3.2. Protocol for Performing an AIMD Simulation

Before performing an AIMD simulation, the size of the system of interest must be decided. In comparison to classical MD simulations, the system size is typically on the order of tens of ionic liquid pairs (Table 1). A well-equilibrated starting configuration is then generated using a classical force field. For most systems, an equilibration run for a few nanoseconds followed by a production run lasting several nanoseconds using the classical force field is sufficient for this purpose. The density of the system is set identical to that measured experimentally or that estimated from a classical isothermal–isobaric ensemble simulation. A reasonably good estimate of the density is required as some ionic liquid properties such as the self-diffusion coefficient depends on the imposed density (see below). Open-source packages such as CP2K [59], CPMD

[60], SIESTA [61], and NWChem [62] are available to the research community for conducting AIMD simulation.

Here we take the example of CP2K code and describe other considerations that must be made prior to an AIMD simulation. In the CP2K code, the QUICKSTEP module uses a hybrid Gaussian and plane wave approach for calculating the energy and its derivatives. The molecularly optimized double-ζ basis set (MOLOPT-DZVP-SR-GTH) is usually selected. Typical density functionals are B3LYP [63, 64] and PBE [65]. The core electrons are treated with Goedecker–Teter–Hutter pseudopotentials [66]. Recently, Grimme's empirical dispersion corrections have also been applied [67]. Additional selections regarding the number of self-consistent field (SCF) cycles for convergence and criteria for convergence are required. AIMD simulations are generally performed under periodic boundary conditions to emulate the macroscopic system. Similar to classical molecular dynamics simulations, an equilibration simulation succeeded by a production run is performed. The temperature of the system is controlled with a thermostat. The output of an AIMD simulation includes the positions and velocities of nuclei as a function of time as well as electronic density from which electronic properties such as partial charges, dipole moment, quadrupole moment and their distributions can be computed.

4. AB INITIO MOLECULAR DYNAMICS OF NEAT IONIC LIQUIDS

The very first AIMD simulations of an ionic liquid was conducted by Del Pòpolo et al. [68]. In this work, the ionic liquid dimethylimidazolium [C_1mim] chloride Cl was simulated to elucidate the structural features of the ionic liquid pair in the gas phase, bulk solid, and liquid. Cation–anion interactions were described in the form of radial distribution functions (RDFs) of the centers of the ions as well as site–site RDFs. It was shown that the ab initio calculations performed by varying the number of ionic liquid pairs (8 and 24) yielded similar structural information. The authors stressed that a relatively short timescale sampled in these simulations was adequate because the initial configuration of the system was taken from a well-equilibrated ionic liquid structure obtained from a force field-based simulation. Holm and coworkers employed CPMD simulations of the ionic liquid [C_1mim]Cl

with 30 ion pairs for approximately 25 ps and performed partial charge analysis with the Blöchl method [69]. Their results indicated that the average charge on the cation and anion was ±0.63e considerably lower than unity, suggesting the importance of polarization and charge transfer in the ionic liquid system. Additionally, the authors noted that the overall charge on the ions was determined to be ±0.82e using the Bader analysis approach. Calculation of overall charge on the ions in an isolated ion pair also yielded a similar value leading the authors to conclude that polarization effects are local in nature [70]. Such simulations provide a justification for the scaling factor applied to the unit charges of cation and anion in force field-based simulations in order to mimic polarization. The authors also compared the partial atomic charges obtained from the bulk CPMD simulation to those from two different force fields and found that notable differences in not only the overall charge on the ions but also at the hydrogen bonding position (see Fig. 1) in the cation. Delle Site and coworkers examined the identical system from the perspective of dipole moments and found that the dipole moment of the anion is about 0.5 D while that of the cation is significantly larger ~2.8 D. More importantly, fluctuations of the dipole moment around the mean are large—approximately half of the mean value suggesting a strong ionic character of the fluid. Additionally, this behavior also implies that classical force fields with fixed charges cannot accurately predict the dielectric properties of ionic liquids. As the ionic dipole moments were found to be a weak function of the number of ionic liquid pairs employed in CPMD simulations, it was also concluded that these properties and the respective fluctuations depend primarily on the local environment of the ion pair [71]. As a side note, dipole moments on the cation and anion were calculated using the localized Wannier scheme incorporated in CPMD. In this approach, the continuous electron distribution is partitioned among all the molecules by localizing the electron density. The dipole moment is then determined by $\boldsymbol{\mu} = \sum_i q_i \boldsymbol{r}_i$, where $\boldsymbol{r}_i$ is the position vector from a reference point to the negative charge centers at which Wannier functions are localized and nuclei carrying the positive charge. In this study, the geometrical center for the cation was chosen as the reference point. As the dipole moment is not uniquely defined for an ion, different reference points such as the center-of-mass or center-of-charge are can be selected.

However, the qualitative trends are not expected to be strongly dependent on the reference point [72].

AIMD simulations performed on three ionic liquids 1-ethyl-3-methylimidazolium [C_2mim] tetracyanoborate [$B(CN)_4$], [C_2mim] dicyanamide [$N(CN)_2$], and [C_2mim] thiocyanate [SCN] showed the expected strong cation–anion interactions in all the ionic liquids. However, the cation–cation π–π interactions usually occurring at ~4 Å were prevalent only in the [C_2mim][SCN] ionic liquid because of the large number of cations (~11) residing in the first solvation shell of the $[C_2mim]^+$ cation. The anion was also found to participate in the cation–π interaction with the highest fraction noted for the [C_2mim][$N(CN)_2$] ionic liquid. Hydrogen bonding between the cation and anion was established through the most acidic hydrogen site and the electronegative N (and S) in the anions. Additionally, the hydrogen atoms in the 3-methyl positions were also seen to be involved in the hydrogen bonding with the anions. The authors also reported a puzzling observation that the diffusion coefficient of the ionic liquid [C_2mim][SCN] was the largest among the three ionic liquids; however, experimentally, the ionic liquid is the most viscous [73].

5. INCLUSION OF DISPERSION CORRECTION

Kirchner and coworkers [74] examined structural and dynamical properties of the ionic liquid [C_2mim] [SCN] in an attempt to evaluate the effect of dispersion corrections while carrying out AIMD calculations. Their results demonstrated that the inclusion of dispersion corrections did not influence the RDFs appreciably. On the other hand, the effect of dispersion corrections led to an enhanced fraction of π–π stacking of the imidazolium rings. The uncorrected AIMD simulation resulted in the self-diffusion coefficients for the anion greater than those for the cation, an observation that is contrary to experimental measurement. Firaha et al. investigated the influence of dispersion corrections on the microheterogeneity of the ionic liquid 1-butyl-3-methylimidazolium [C_4mim] trifluorosulfonate [CF_3SO_3] with AIMD calculations using the BLYP and BLYP-D3 functionals. Contrary to chemical intuition, the inclusion of dispersion correction resulted in a decrease in the microheterogeneity of the system indicated by lowering of the first peak height in the RDFs of alkyl chain units. The authors also reported

enhanced interactions of the anion with alkyl groups when dispersion corrections are applied [75]. Perlt et al. concluded that the structural quantities such as the RDFs and structure factors predicted from the classical simulations and AIMD simulations with revPBE-D3 and OLYP-D3 functionals are in good agreement. The classical simulations, however, predict hydrogen bonds that are longer and more bent in comparison to those observed in the AIMD calculations [67].

6. PROPERTIES FROM AIMD SIMULATIONS VS MD SIMULATIONS

Bhargava and Balasubramanian carried out CPMD simulations of the ionic liquid [C_1mim] Cl at 425 K with 32 ionic liquid pairs along with MD simulations of the same ionic liquid with the objective of comparing the intermolecular structures obtained with the two methods. The structure expressed in terms of the RDFs of the center-of-mass of ions was nearly identical; however, a shortening of the peak distance in the RDFs between the ring hydrogen atoms and chloride was noted in the CPMD calculations. The results indicated the need for refinement in the interatomic potential to describe such a behavior [76]. The same authors reported the structure of the ionic liquid [C_4mim] hexafluorophosphate [PF_6] obtained from CPMD simulations. A comparison of the center-of-mass (COM) RDF between CPMD and MD simulations showed that the anions are able to approach closer in the CPMD simulations due to electronic polarizability. In the same study, the authors investigated the effect of the presence of CO_2 in this ionic liquid. The addition of CO_2 was found to result in the decrease in the anion–anion coordination number in the first solvation as a result of the anion–CO_2 interactions. Examination of the RDF between CO_2 and the acidic proton revealed cation–CO_2 interactions which was absent in RDFs extracted from MD simulations [77]. A similar observation was reported from the AIMD study involving 1 CO_2 molecule dissolved in 36 ionic liquid pairs of [C_2mim] acetate [CH_3COO] under periodic boundary conditions that the cation contributes significantly to the solvent–solute interactions [78]. Furthermore, the results from the AIMD simulations demonstrated the bending of the CO_2 molecule when dissolved in this ionic liquid. The importance of such studies is underscored by the fact that the force field-based simulations are generally performed with

rigid representation of CO_2 molecules eliminating the possibility of observing the bending of CO_2 molecules. AIMD simulations can also provide an explanation for the high solubility of SO_2 in $[C_2mim][SCN]$ ionic liquid. An AIMD solvation study of SO_2 in this ionic liquid suggested that SO_2 is actually accommodated in the ionic liquid network due to its participation in synergistic interactions with both the cation and anion of the ionic liquid [79].

Generally, the number of ionic liquid pairs in AIMD simulations tends to be 32; however, recently, Nagata and coworkers performed AIMD simulations on a relatively large number of ionic liquid pairs (70 and 120) for the ionic liquid $[C_2mim]Cl$. The objective of this work was to investigate the effect of two different functionals on the ionic liquid–vacuum and ionic liquid–graphene interfacial structures [80]. A notable observation in this study was that the decay of the difference in the cation and anion charge density from the interface to the bulk was slower than that predicted by a polarizable force field and was similar to that obtained from force field-based simulations. The authors demonstrated that a higher preference for parallel stacking of imidazolium rings induced by π–π interactions at the interface is responsible for the slower decay of the net positive charge density away from the interface. Further, it was demonstrated that the PBE functional with Grimme-D3 corrections underpredicted the formation of π–π-stacked structures in comparison to that predicted by the BLYP-D3-AIMD simulations as the former is known to lower the binding energy for such conformations, underscoring the need for an appropriate level of theory in modeling ionic liquid systems with AIMD calculations. The π–π interactions also were found to overcome the electrostatic repulsion between neighboring $[C_1mim]^+$ cations in $[C_1mim]$ oxalatoborate [BOB] ionic liquid probed with AIMD. The presence of the oxalato ring also led to the π–π interactions of the anion with the imidazolium plane of the cation. Additionally, the hydrogen bonding interaction of the anion oxygen and the acidic hydrogen atom of the cation enabled parallel displaced stacking conformations at short distances. The imidazolium and oxalato ring planes were observed to adopt perpendicular conformations, stabilized by attractive Coulombic interactions, at long distances [81].

The interfacial structure of the ionic liquid $[C_2mim][CH_3COO]$ droplets of increasing sizes (1 ionic liquid pair to 16 ionic liquid pairs)

was recently investigated by Brehm and Sebastiani using AIMD simulations. Their calculations indicated that the mass density of these clusters is considerably higher than the bulk density of the ionic liquid. The hydrogen bonding was found to be very strong for the isolated ionic liquid pair and decrease with increase in the size of the ionic liquid cluster. However, a very unusual lifetime of ~2000 ps was determined for the 16 ionic liquid pair cluster. The interface of these clusters was observed to present a very hydrophobic surface to vacuum [82].

AIMD simulations can point to features that cannot be captured in classical MD simulations. For example, the short-range structure of the protic ionic liquid cholinium [Ch] norvaline [norval], predicted by classical MD methodology, includes predominantly cation–anion and cation–cation contacts. On the other hand, the structure obtained from AIMD simulations is at odds with the MD simulation results such that the anion–anion are the most prevalent contacts followed by those between cation–cation and cation–anion. Thus, AIMD simulations are able to disclose complex formation involving like-charged species—an observation reported for the very first time in the ionic liquid literature. The study also underscores the importance of explicitly accounting for electronic degrees of freedom to discern such effects [83]. A similar study involving 11 amino acid anions in combination with the cholinium cation was carried out in which the ionic liquids were handled at the ab initio level. The structural analysis of the ionic liquids yielded a general and consistent pattern in which the hydroxyl group of the cation participates in the hydrogen bonding interaction with the carboxylate group of the anion. Such an interaction leaves the positively charged nitrogen atom of the head of the cation to establish additional hydrogen bonding interactions with the carboxylate moiety of another anion. The structural motif pervades throughout the ionic liquid system. Additionally, the authors showed that the calculated X-ray structure factors gathered from the AIMD simulations were in excellent agreement with those collected experimentally. The AIMD treatment of [Ch]cysteinate[Cys] ionic liquid raised the possibility of the transfer of the –SH proton resulting in the formation of a zwitterionic anion, once again showing that AIMD simulations can reveal phenomena not accessible to classical simulation methodologies [84].

For imidazolium-based ionic liquids containing long alkyl chains, it is typical to observe nanoscale segregation of polar and nonpolar do-

mains due to the aggregation of alkyl chains. In small- and wide-angle X-ray scattering patterns, alternating polar–nonpolar domains emerge as a peak in the low-Q region (~0.3–0.4 $Å^{-1}$). Recently, it was demonstrated that the presence of an alkyl chain is not a prerequisite for observing such domains. For example, long-range order is established in the ionic liquid cholinium prolinate, which was confirmed by WAXS and SAXS experiments. Although both MD and AIMD simulations predict the experimental structure factor accurately, the agreement is superior with AIMD predictions. Furthermore, the simulations show that the origin of the long-range order in the ionic liquid stems from a strong hydrogen bonding network resulting from the interaction of the hydroxyl oxygen in the cation and carboxylate oxygen in the anion [85]. In the case of the cholinium cation paired with carboxylate anions such as formate, propionate, and butanoate, the X-ray diffraction patterns obtained from MD simulations do not match the experimental data as the two-body force field derived from Generalized Amber Force Field (GAFF) predicts a stronger hydrogen bonding interaction between the hydroxyl oxygen atom of cholinium and carboxylate oxygen of the anion. Introduction of a three-body hydrogen bonding term in the force field wakens the hydrogen bonding interaction leading to a good agreement of the X-ray diffraction spectra with experimental data. The agreement, however, is not quantitative as the intensities of all the peaks but those arising from intramolecular interactions are not reproduced with the refined force field. On the other hand, AIMD simulations are able to reproduce both the experimental peak positions and intensities. The authors of the study remarked that the structures of these ionic liquids are dictated by a balance of hydrogen bonding and Coulombic interactions in conjunction with conformations adopted by the cholinium cation. In such instances, the quantum-level treatment of the ionic liquids may be superior to a two-body force field-based simulation [86].

Pentylammonium nitrate was also investigated with AIMD simulations from which the wide-angle X-ray scattering profile of the ionic liquid was generated. A good agreement of the profile with experimental results was obtained. The coordination number of oxygen surrounding the ammonium head was calculated to be 5.3, while the number of hydrogen bonds was found to be 2.6, indicating that the positively charged group can participate in more than one hydrogen bond simulta-

neously, but not all oxygen atoms can hydrogen bond with the cations. Thus, the hydrogen bond network of the anions in incomplete [87].

7. AIMD SIMULATIONS OF THE IONIC LIQUID–ELECTRODE INTERFACE

Ionic liquids are ideal candidates for their applications in batteries due to essentially nonvolatile character. The inert nature of many ionic liquids over a wide electrochemical window is another attractive feature. As the formation of the solid electrolyte interface is crucial in protecting the electrode against undesirable chemical reactions, AIMD simulations have been attempted in an effort to provide a microscopic understanding of this process. We outline a representative sampling of the literature in this domain. Typically, a single ion pair is placed in the vicinity of the electrode of interest. In order to simulate the cathode or anode, a positive or negative charge can be introduced on the electrode surface. The extent of bias can be controlled by manipulating the magnitude of the excess charge placed on the electrode. During the course of a simulation, charges on the ionic liquid cation and anion are monitored to provide clues for the propensity for reduction or oxidation.

Following this methodology, Otani and coworkers performed an AIMD simulation of *N*-methyl-*N*-propylpiperidinium [PP13] bis(trifluoromethanesulfonyl)imide [NTf_2] ionic liquid in the presence of nickel and lithium electrodes. The ionic liquid remained stable at the nickel interface during a 1 ps simulation when the system carried an excess charge of −1e. Under the positive bias of +1e charge on the nickel electrode, the overall charge on the anion was found to be −0.58e, while the cation charge increased to 1.07e, implying that the charge transfer occurred to both the ions. However, the anion decomposed as the excess charge increased to +2e. The overall charge on the anion reached a value close to zero, indicating that the anion was oxidized. Additionally, anion decomposition occurred via the breakage of an S–C bond. In contrast, the anion is reduced when placed in contact with a lithium surface under both positive and negative bias. In fact, the reduction of the anion is accompanied by the anion decomposition, which leads to the release of fluorine atom and the formation of LiF passivating the electrode [88]. In another publication, ab initio calculations performed with plane wave DFT implemented in VASP were employed to understand

the initial stages of the ionic liquid [PP13][NTf_2] decomposition on a Li surface. The calculations permitted identification of species such as LiF, Li_2F, LiO, and Li_2O in the SEI layer, the presence of which was confirmed by XPS analysis. During the course of the simulation, no breakdown of the cation was noticed; however, the experiments, conducted over longer time scales, provided evidence that the cation undergoes chemical reaction at the interface [89].

Lawson and coworkers investigated in great detail the decomposition of two ionic liquids: butylmethylpyrrolidinium [Pyr14][NTf_2] and [C_2mim][BF_4] using AIMD simulations. One of the notable features of these calculations is that the authors considered different cation–anion configurations on the Li (100) surface. Additionally, the authors also probed the Li–ionic liquid interface taking into consideration bulk ionic liquid in contact with the Li surface. The ionic liquid [C_2mim][BF_4] displayed stability toward decomposition and the initial stages of the reaction with Li could be observed only at a very high temperature of 2500 K. On the other hand, breakdown of the anion $[NTf_2]^-$ could be initiated at room temperature. The cation in both ionic liquids did not generate any decomposition products. As deduced in earlier studies, the charge transfer from Li to $[NTf_2]^-$ was shown to be responsible for the breakdown of the anion. The initial steps consisted of the cleavage of C–S and/or S–N producing species such as LiF, LiO, Li_2F, Li_2O, and SO_2. For the single ion pair AIMD simulation, no F abstraction event appeared. However, the solvation of interfacial ionic liquid pairs by the bulk induced several long-lived F binding anions which then resulted in the reaction of F with Li underscoring the importance of the bulk in such calculations. It is to be noted that the extraction of fluorine is possible when the electrode is charged as outlined earlier [90].

8. AIMD SIMULATIONS OF BINARY IONIC LIQUID MIXTURES

Kirchner and coworkers examined an equimolar mixture of [C_2mim]Cl and [C_2mim][SCN] and the pure ionic liquids with AIMD simulations. The authors fully characterized structures of these systems and concluded that the stronger interacting anion Cl^- displaces the coordination of sulfur atom in $[SCN]^-$ from the association site with the cation. The neighboring imidazolium rings were found to locate paral-

lel to each other due to π–π interactions. The study also demonstrated that the self-diffusion coefficients of the ions are a strong function of the densities of the examined mixtures. The different coordination of the anions around the cation was also reflected in the computed power spectra of the mixture, which deviated from those of the pure ionic liquid spectra in the region corresponding to the imidazolium ring hydrogen atoms [91].

Very recently, Macchieraldo et al. [92] performed AIMD simulations of binary ionic liquid mixtures composed of $[C_4mim]Cl$ and $[C_4mim][BF_4]$ with and without water. The authors selected an AIMD-based approach to account for charge transfer and polarization. RDF analysis showed that the number of anions surrounding a cation mirrors the molar ratio of the binary ionic liquid mixture when water is not present in the system. However, the addition of water shifts this balance in favor of $[BF_4]^-$ such that approximately three $[BF_4]^-$ anions are found for every Cl^- in the first solvation shell of the cation. The presence of water "solubilizes" the Cl^- anion while the ionic liquid network is maintained through the coordination of the cation with $[BF_4]^-$. A charge analysis carried out for the two systems revealed that the charge distributions of the ions differ considerably from the unity and that these distributions are reminiscent of a Gaussian distribution. Furthermore, a more detailed analysis of the charge distribution on the various methyl and methylene groups of the cation demonstrated two important aspects: (1) there is a distribution of charges and (2) the positions of the maximum in these distributions are different from the widely used Lopes and Pàdua force field [34]. CPMD simulations of the ionic liquid $[C_4mim][PF_6]$ and $[C_4mim][BF_4]$ and their mixtures with water in a 1:3 molar ratio indicated that a charge transfer takes place from ionic liquid to water molecules such that water molecules acquire a negative charge. The binary mixture of water with more hydrophilic ionic liquid showed a greater charge transfer to water molecules. The average dipole moment of water in these systems was found to be ~2.32 D with $[C_4mim][BF_4]$ and 2.42 D when mixed with $[C_4mim][PF_6]$—values considerably lower than the 2.85 D for bulk water [93]. Similarly, depolarization of water molecules in the ionic liquid monomethylammonium nitrate was observed from a CPMD simulation involving 48 ionic liquid pairs and 4 water molecules [94]. Based on the computation of water isotherms in three ionic liquids, Marin-Rimoldi et al. [95] also

suggested that ionic liquid-dependent scaling factors are required to match the simulation predictions of water solubility with those measured experimentally and that improved force field taking into account the charge transfer and polarization are necessary for ionic liquid–water systems.

In order to elucidate solvation of water and CO_2 in ionic liquids, Rezabal and Schäfer simulated one solute molecule in 18 $[C_1mim]Cl$ ionic liquid using an AIMD method. The analysis of trajectories for the water–ionic liquid system indicated that the hydrogen bond network of water is fully saturated: two hydrogen atoms (H_W) in water interact with Cl^- anion while the oxygen atom (O_W) coordinates with ring hydrogen atoms on the other side of the most acidic proton in the cation. When these interactions are analyzed in terms of noncovalent index, it was revealed that the H_W–Cl^- interaction remained stable during the course of the simulation; however, the structuring around O_W exhibited flexibility. The authors also noted nonspecific interactions of water with the methyl groups. CO_2, on the other hand, displays much weaker interactions with both the cation and anion. Each oxygen atom in CO_2 interacts with two cations yielding a total of four cations in the solvation shell of CO_2. As opposed to this, only 1.5 Cl^- anions are present in the coordination shell of CO_2. Thus, it was concluded that the cations contribute to a greater extent than the anion in this particular ionic liquid. The study clearly demonstrates that although the CO_2 solubility in ionic liquids is predominantly anion-dependent [96, 97], dispersion interactions with the cation cannot be neglected [98]. In a CPMD study carried out by Bhargava et al. on the ionic liquid $[C_4mim][PF_6]$-CO_2 mixture, the authors reported a similar observation that CO_2 interacts with the imidazolium ring carbon atom connected to the most acidic hydrogen atom. Interestingly, the authors also identified a significant interaction of CO_2 with the terminal carbon atom in the butyl chain from the calculated RDFs [99].

Three mixtures of cholinium phenylalaninate with water in the molar ratio 4:1, 1:1.5, and 1:9 were studied by AIMD simulations by Gontrani et al. [100]. The authors found that the experimental structure factors and RDFs could be accurately reproduced in simulations. The hydrogen bonding between the cation and anion persisted in three mixtures investigated. Hydrogen bonding interactions of the hydroxyl group of the cation with water were also noted. It was discovered that

at high water concentrations (molar ratio 1:9), water molecules act as mediators of the cation–anion interactions.

9. ELECTROCHEMICAL WINDOW OF IONIC LIQUIDS AND GROTTHUSS-TYPE MECHANISM

Ionic liquids, due to their electrochemical stability, are considered promising electrolytes in Li-ion batteries. AIMD simulations can provide useful insight into the electrochemical stability of ionic liquids and the charge transport in them. As an example, Maginn and coworkers utilized AIMD calculations to compute the highest occupied molecular orbital (HOMO) and lowest occupied molecular orbital energies (LUMO) of the snapshots generated from MD simulations of a number of ionic liquids. Instead of calculating the HOMO and LUMO energies by performing a single-point calculations at a quantum level, the snapshots were relaxed using CPMD simulations for 300 steps with the final configuration quenched to an energy minimum. The authors found that the energy relaxation using CPMD led to a better prediction of the electrochemical window for a range of ionic liquids than those obtained with the single-point energy calculation [101].

In some ionic liquids, the charge transport occurs via the Grotthuss mechanism usually invoked to explain the facilitated transfer of the proton in which the proton movement in liquid water is accomplished by hopping from one water molecule to another along a hydrogen-bonded network [102, 103]. McDaniel and Yethiraj employed AIMD simulations to provide a theoretical description of the empirically proposed Grotthuss-type charge transport mechanism in $[C_2mim]/I_3$ crystals, involving I^- and I_3^-. The potential of mean force calculations for the association and dissociation of the two species indicated that the exchange is thermally facile with free energy barrier of 1–2 kcal/mol [104]. AIMD calculations have also been applied to understand proton-transfer mechanism in both aprotic and protic ionic liquids. Very recently, Kirchner and coworkers performed AIMD simulations on the equimolar mixture of *N*-methylimidazole and acetic acid. Based on the RDFs, the authors extracted the proton coordination numbers and reported, for the first time, ionicity of the protic ionic liquid computationally. Their calculations suggested low ionicity of the ionic liquid; however, the analysis of the AIMD trajectories of several tens of picosec-

onds revealed that the Grotthuss-type mechanism was operative yielding similar self-diffusion coefficient of the neutral species and the mobile proton. The authors also generated a large number of theoretical candidates for designing superionic protic ionic liquids by substituting the ring hydrogens in the cation *N*-methylimidazolum and the $-CH_3$ hydrogens in acetate and conducted static quantum calculations to compute the Gibbs free energy of transfer of the proton from the cation to the anion resulting into neutral species. These calculations enabled the authors to conclude that the Gibbs free energy change from −45 to 45 kJ/mol is desirable for the Grotthuss-enabled proton transport [105]. Cholinium aspartate represents another interesting system in which the Grotthuss-type mechanism was discovered by Bodo and coworkers who conducted AIMD simulations of the ionic liquid. The proton transfer, in this ionic liquid, occurs from the carboxylate group of one anion to the amino group of the other. The calculations also suggested that the cation participates, at least on the simulation time scale, as a mere spectator for the proton conduction [106]. Due to the fixed chemical identity of the ions in MD simulations, the migration of the proton within an ion or between ions cannot be captured.

10. SUMMARY AND OUTLOOK

AIMD simulations are now becoming a mainstream research tool not only for understanding microscopic structure of fascinating ionic liquids, but also designing novel ionic liquids, thus enabling us to truly harness the designer capability of a large number of cations and anions. One of the main advantages of AIMD calculations is that the extensive parametrization necessary to benchmark a force field for a classical molecular simulation is not required. Furthermore, due to the explicit treatment of electrons, important chemical phenomena such as intermolecular and intramolecular hydrogen transfer, formation of solute driven adducts, and reactions of ionic liquids with acidic gases such as CO_2 can be captured. The handling of the system at the electronic level, however, leads to such calculations requiring access to significant computational resources. The high computational cost usually is a limiting factor for the system size (length scales) and simulation length (time scales) accessible to AIMD calculations. Based on our survey of the literature, there is only one system for which the number of ionic liquid

pairs exceeds 100, while most simulations have been performed on system sizes on the order of tens of cation–anion pairs. Similarly, very few simulations have achieved sampling beyond 100 ps (see Table 1). As the literature contains numerous examples of ionic liquids for which the nanoscale heterogeneity is present at several nanometers, such phenomena cannot be probed, at present, with AIMD methodology. Similarly, the computation of transport properties such as viscosity of ionic liquids requiring long simulation times are currently beyond the reach of AIMD calculations. However, we believe that combination of AIMD simulations to access the local structure of ionic liquids supplemented by force field-based molecular dynamics and MC simulation methodologies can be applied to cover a broad range of length scales and time scales necessary to probe a large number of electronic, thermophysical and phase-equilibria properties in ionic liquids.

ACKNOWLEDGMENT

The author gratefully acknowledges funding from the National Science Foundation (NSF) Award Number CBET-1706978 for this work.

REFERENCES

1. S. Gabriel, J. Weiner, Ueber Einige Abkömmlinge Des Propylamins, Chem. Ber. 21 (1888) 2669–2679.
2. P. Walden, Molecular Weights and Electrical Conductivity of Several Fused Salts, Bull. Russ. Acad. Sci. (1914) 405–422.
3. H.L. Chum, V.R. Koch, L.L. Miller, R.A. Osteryoung, Electrochemical Scrutiny of Organometallic Iron Complexes and Hexamethylbenzene in a Room Temperature Molten Salt, J. Am. Chem. Soc. 97 (11) (1975) 3264–3265.
4. J.S. Wilkes, J.A. Leviskly, R.A. Wilson, C.L. Hussey, Dialkylimidazolium Chloroaluminate Melts: A New Class of Room-Temperature Ionic Liquids for Electrochemistry, Spectroscopy and Synthesis, Inorg. Chem. 21 (1982) 1263–1264.
5. R.J. Gale, R.A. Osteryoung, Potentiometric Investigation of Dialuminum Heptachloride Formation in Aluminum Chloride-1-Butylpyridinium Chloride Mixtures, Inorg. Chem. 18 (1979) 1603–1605.
6. J.S. Wilkes, M.J. Zaworotko, Air and Water Stable 1-Ethyl-3-methylimidazolium Based Ionic Liquids, J. Chem. Soc. Chem. Commun. (13) (1992) 965–967.
7. https://www.Chem.info/news/2016/10/chevron-and-honeywell-switch-revolutionary-alkylation-technology.
8. M. Abai, M.P. Atkins, A. Hassan, J.D. Holbrey, Y. Kuah, P. Nockemann, A.A. Oliferenko, N.V. Plechkova, S. Rafeen, A.A. Rahman, R. Ramli, S.M. Shariff, K.R. Seddon, G. Srinivasan, Y. Zou, An Ionic Liquid Process for Mercury Removal From Natural Gas, Dalton Trans. 44 (18) (2015) 8617–8624.

9. L.M. Sidisky, M.D. Buchanan, Supelco Patented Ionic Liquid GC Phase Technology, Supelco Reporter 26 (2008) 3–4.
10. U. Kapoor, J.K. Shah, Thermophysical Properties of Imidazolium-Based Binary Ionic Liquid Mixtures Using Molecular Dynamics Simulations, J. Chem. Eng. Data 63 (7) (2018) 2512–2521.
11. U. Kapoor, J.K. Shah, Preferential Ionic Interactions and Microscopic Structural Changes Drive Nonideality in the Binary Ionic Liquid Mixtures as Revealed From Molecular Simulations, Ind. Eng. Chem. Res. 55 (2016) 13132–13146.
12. G. Chatel, J.F.B. Pereira, V. Debbeti, H. Wang, R.D. Rogers, Mixing Ionic Liquids – "Simple Mixtures" or "Double Salts"?, Green Chem. 16 (4) (2014) 2051–2083.
13. J.L. Anthony, E.J. Maginn, J.F. Brennecke, Solubilities and Thermodynamic Properties of Gases in the Ionic Liquid 1-n-Butyl-3-methylimidazolium Hexafluorophosphate, J. Phys. Chem. B 106 (29) (2002) 7315–7320.
14. Z. Lei, C. Dai, B. Chen, Gas Solubility in Ionic Liquids, Chem. Rev. 114 (2) (2014) 1289–1326.
15. J.E. Bara, T.K. Carlisle, C.J. Gabriel, D. Camper, A. Finotello, D.L. Gin, R.D. Noble, Guide to CO_2 Separations in Imidazolium-Based Room-Temperature Ionic Liquids, Ind. Eng. Chem. Res. 48 (6) (2009) 2739–2751.
16. D. Almantariotis, S. Stevanovic, O. Fandiño, A.S. Pensado, A.A.H. Padua, J.Y. Coxam, M.F. Costa Gomes, Absorption of Carbon Dioxide, Nitrous oxide, Ethane and Nitrogen by 1-Alkyl-3-methylimidazolium ($C_n$mim, n = 2,4,6) Tris(pentafluoroethyl)trifluorophosphate Ionic Liquids (eFAP), J. Phys. Chem. B 116 (26) (2012) 7728–7738.
17. M. Bidikoudi, T. Stergiopoulos, V. Likodimos, G.E. Romanos, M. Francisco, B. Iliev, G. Adamová, T.J.S. Schubert, P. Falaras, Ionic Liquid Redox Electrolytes Based on Binary Mixtures of 1-Alkyl-methylimidazolium tricyanomethanide With 1-Methyl-3-propylimidazolium Iodide and Implication in Dye-Sensitized Solar Cells, J. Mater. Chem. A 1 (35) (2013) 10474–10486.
18. C. Pinilla, M.G. Del Popolo, R.M. Lynden-Bell, J. Kohanoff, Structure and Dynamics of a Confined Ionic Liquid. Topics of Relevance to Dye-Sensitized Solar Cells, J. Phys. Chem. B 109 (38) (2005) 17922–17927.
19. P. Wang, S.M. Zakeeruddin, J.E. Moser, M. Grätzel, A New Ionic Liquid Electrolyte Enhances the Conversion Efficiency of Dye-Sensitized Solar Cells, J. Phys. Chem. B 107 (48) (2003) 13280–13285.
20. P. Wasserscheid, W. Keim, Ionic Liquids–New "Solutions" for Transition Metal Catalysis, Angew. Chem. Int. Ed. 39 (21) (2000) 3772–3789.
21. A. Riisagera, R. Fehrmanna, M. Haumannb, P. Wasserscheidb, Supported Ionic Liquids: Versatile Reaction and Separation Media, Top. Catal. 40 (1–4) (2006) 91–102.
22. G.H. Lane, P.M. Bayley, B.R. Clare, A.S. Best, D.R. Macfarlane, M. Forsyth, A.F. Hollenkamp, Ionic Liquid Electrolyte for Lithium Metal Batteries: Physical, Electrochemical, and Interfacial Studies of n-Methyl-n-butylmorpholinium Bis(fluorosulfonyl)imide, J. Phys. Chem. C 114 (49) (2010) 21775–21785.
23. L.T. Costa, B. Sun, F. Jeschull, D. Brandell, Polymer-Ionic Liquid Ternary Systems for Li-Battery Electrolytes: Molecular Dynamics Studies of LiTFSI in a EMIm-TFSI and PEO Blend, J. Chem. Phys. 143 (2) (2015), 024904-1-024904-9.

24. A. Basile, H. Yoon, D.R. MacFarlane, M. Forsyth, P.C. Howlett, Investigating Non-Fluorinated Anions for Sodium Battery Electrolytes Based on Ionic Liquids, Electrochem. Commun. 71 (2016) 48–51.

25. J. Szymczak, S. Legeai, S. Michel, S. Diliberto, N. Stein, C. Boulanger, Electrodeposition of Stoichiometric Bismuth Telluride Bi2Te3 Using a Piperidinium Ionic Liquid Binary Mixture, Electrochim. Acta 137 (2014) 586–594.

26. Z. Liu, T. Cui, T. Lu, M. Shapouri Ghazvini, F. Endres, Anion Effects on the Solid/Ionic Liquid Interface and the Electrodeposition of Zinc, J. Phys. Chem. C 120 (2016) 20224–20231.

27. J. Liu, G. Jiang, J. Jönsson, Application of Ionic Liquids in Analytical Chemistry, Trends Anal. Chem. 24 (1) (2005) 20–27.

28. V. Pino, A.M. Afonso, Surface-Bonded Ionic Liquid Stationary Phases in High-Performance Liquid Chromatography—A Review, Anal. Chim. Acta 714 (2012) 20–37.

29. N. Plechkova, K. Seddon, Applications of Ionic Liquids in Chemical Industry, Chem. Soc. Rev. 37 (2008) 123–150.

30. J.K. Shah, J.F. Brennecke, E.J. Maginn, Thermodynamic Properties of the Ionic Liquid 1-n-Butyl-3-methylimidazolium Hexafluorophosphate From Monte Carlo Simulations, Green Chemistry 4 (2) (2002) 112–118.

31. C. Cadena, E.J. Maginn, Molecular Simulation Study of Some Thermophysical and Transport Properties of Triazolium-Based Ionic Liquids, J. Phys. Chem. B 110 (36) (2006) 18026–18039.

32. J.N.C. Lopes, J. Deschamps, A.A.H. Padua, Modeling Ionic Liquids Using a Systematic All-Atom Force Field, J. Phys. Chem. B 108 (6) (2004) 2038–2047.

33. J.N. Canongialopes, A.A.H. Padua, Molecular Force Field for Ionic Liquids Composed of Triflate or Bistriflylimide Anions, J. Phys. Chem. B 108 (43) (2004) 16893–16898.

34. J.N.C. Lopes, A.A.H. Pádua, Molecular Force Field for Ionic Liquids III: Imidazolium, Pyridinium, and Phosphonium Cations; Chloride, Bromide, and Dicyanamide Anions, J. Phys. Chem. B 110 (39) (2006) 19586–19592.

35. J.N.C. Lopes, A.A.H. Padua, K. Shimizu, Molecular Force Field for Ionic Liquids IV: Trialkylimidazolium and Alkoxycarbonyl-Imidazolium Cations; Alkylsulfonate and Alkylsulfate Anions, J. Phys. Chem. B 112 (16) (2008) 5039–5046.

36. K. Shimizu, D. Almantariotis, M.F.C. Gomes, A.A.H. Pádua, J.N.C. Lopes, Molecular Force Field for Ionic Liquids V: Hydroxyethylimidazolium, Dimethoxy-2-methylimidazolium, and Fluoroalkylimidazolium Cations and Bis(fluorosulfonyl)amide, Perfluoroalkanesulfonylamide, and Fluoroalkylfluorophosphate Anions, J. Phys. Chem. B 114 (10) (2010) 3592–3600.

37. X. Zhong, Z. Liu, D. Cao, Improved Classical United-Atom Force Field for Imidazolium-Based Ionic Liquids: Tetrafluoroborate, Hexafluorophosphate, Methylsulfate, Trifluoromethylsulfonate, Acetate, Trifluoroacetate, and Bis(trifluoromethylsulfonyl)amide, J. Phys. Chem. B 115 (33) (2011) 10027–10040.

38. B. Doherty, X. Zhong, O. Acevedo, A Virtual Site OPLS Force Field for Imidazolium-Based Ionic Liquids, J. Phys. Chem. B 122 (2018) 2962–2974.

39. B. Doherty, X. Zhong, S. Gathiaka, B. Li, O. Acevedo, Revisiting OPLS Force Field Parameters for Ionic Liquid Simulations, J. Chem. Theor. Comput. 13 (12) (2017) 6131–6145.

40. S.V. Sambasivarao, O. Acevedo, Development of OPLS-AA Force Field Parameters for 68 Unique Ionic Liquids, J. Chem. Theor. Comput. 5 (4) (2009) 1038–1050.

41. T. Köddermann, D. Paschek, R. Ludwig, Molecular Dynamic Simulations of Ionic Liquids: A Reliable Description of Structure, Thermodynamics and Dynamics, ChemPhysChem 8 (17) (2007) 2464–2470.

42. K.G. Sprenger, V.W. Jaeger, J. Pfaendtner, The General Amber Force Field (GAFF) Can Accurately Predict Thermodynamic and Transport Properties of Many Ionic Liquids, J. Phys. Chem. B 119 (18) (2015) 5882–5895.

43. S. Plimpton, Fast Parallel Algorithms for Short-Range Molecular Dynamics, J. Comput. Phys. 117 (1) (1995) 1–19.

44. M.J. Abraham, T. Murtola, R. Schulz, S. Páll, J.C. Smith, B. Hess, E. Lindahl, GROMACS: High Performance Molecular Simulations Through Multi-Level Parallelism From Laptops to Supercomputers, SoftwareX 1–2 (2015) 19–25.

45. J.C. Phillips, R. Braun, W. Wang, J. Gumbart, E. Tajkhorshid, E. Villa, C. Chipot, R.D. Skeel, L. Kalé, K. Schulten, Scalable Molecular Dynamics With NAMD, J. Comput. Chem. 26 (16) (2005) 1781–1802.

46. I.T. Todorov, W. Smith, K. Trachenko, M.T. Dove, DL_POLY_3: New Dimensions in Molecular Dynamics Simulations Via Massive Parallelism, J. Mater. Chem. 16 (20) (2006) 1911–1918.

47. N. Metropolis, A.W. Rosenbluth, M.N. Rosenbluth, A.H. Teller, Equations of State Calculations by Fast Computing Machines, J. Chem. Phys. 21 (1853) 1087–1092.

48. J.K. Shah, E. Marin-Rimoldi, R.G. Mullen, B.P. Keene, S. Khan, A.S. Paluch, N. Rai, L.L. Romanielo, T.W. Rosch, B. Yoo, E.J. Maginn, Cassandra: An Open Source Monte Carlo Package for Molecular Simulation, J. Comput. Chem. 38 (19) (2017) 1727–1739.

49. M.G. Martin, MCCCS Towhee: A Tool for Monte Carlo Molecular Simulation, Mol. Simul. 39 (14–15) (2013) 1212–1222.

50. Y. Wang, S. Feng, G.A. Voth, Transferable Coarse-Grained Models for Ionic Liquids, J. Chem. Theor. Comput. 5 (4) (2009) 1091–1098.

51. B.L. Bhargava, R. Devane, M.L. Klein, S. Balasubramanian, Nanoscale Organization in Room Temperature Ionic Liquids: A Coarse Grained Molecular Dynamics Simulation Study, Soft Matter 3 (11) (2007) 1395–1400.

52. B. Yoo, Y. Zhu, E.J. Maginn, Molecular Mechanism of Ionic-Liquid-Induced Membrane Disruption: Morphological Changes to Bilayers, Multilayers, and Vesicles, Langmuir 32 (21) (2016) 5403–5411.

53. H. Liu, E. Maginn, A Molecular Dynamics Investigation of the Structural and Dynamic Properties of the Ionic Liquid 1-n-butyl-3-methylimidazolium Bis(trifluoromethanesulfonyl)imide, J. Chem. Phys. 135 (12) (2011), 124507-1-124507-16.

54. D. Bedrov, O. Borodin, Z. Li, G.D. Smith, Influence of Polarization on Structural, Thermodynamic, and Dynamic Properties of Ionic Liquids Obtained From Molecular Dynamics Simulations, J. Phys. Chem. B 114 (15) (2010) 4984–4997.

55. O. Borodin, Polarizable Force Field Development and Molecular Dynamics Simulations of Ionic Liquids, J. Phys. Chem. B 113 (33) (2009) 11463–11478.

56. C. Schröder, Comparing Reduced Partial Charge Models With Polarizable Simulations of Ionic Liquids, Phys. Chem. Chem. Phys. 14 (9) (2012) 3089.

57. C. Schröder, O. Steinhauser, Simulating Polarizable Molecular Ionic Liquids With Drude Oscillators, J. Chem. Phys. 133 (15) (2010), 154511-1-154511-13.

58. R. Car, M. Parrinello, Unified Approach for Molecular Dynamics and Density-Functional Theory, Phys. Rev. Lett. 55 (22) (1985) 2471–2474.

59. www.cp2k.org.

60. www.cpmd.org.

61. J.M. Soler, E. Artacho, J.D. Gale, A. García, J. Junquera, P. Ordejón, D. Sánchez-Portal, The SIESTA Method for Ab Initio Order-N Materials Simulation, J. Phys. Condens. Matter 14 (11) (2002) 2745–2779.

62. M. Valiev, E.J. Bylaska, N. Govind, K. Kowalski, T.P. Straatsma, H.J.J. Van Dam, D. Wang, J. Nieplocha, E. Apra, T.L. Windus, W.A. de Jong, NWChem: A Comprehensive and Scalable Open-Source Solution for Large Scale Molecular Simulations, Comput. Phys. Commun. 181 (9) (2010) 1477–1489.

63. C. Lee, W. Yang, R.G. Parr, Development of the Colle-Salvetti Correlation-Energy Formula Into a Functional of the Electron Density, Phys. Rev. B 37 (2) (1988) 785–789.

64. A.D. Becke, Density-Functional Exchange-Energy Approximation With Correct Asymptotic Behavior, Phy. Rev. A 38 (6) (1988) 3098–3100.

65. J.P. Perdew, J.A. Chevary, S.H. Vosko, K.A. Jackson, M.R. Pederson, S.D. J, C. Fiolhais, Atoms, Molecules, Solids, and Surfaces: Applications of the Generalized Gradient Approximation for Exchange and Correlation, Phys. Rev. B 46 (11) (1992) 6671–6687.

66. S. Goedecker, M. Teter, J. Hutter, Separable Dual-Space Gaussian Pseudopotentials, Phys. Rev. B 54 (3) (1996) 1703–1710.

67. E. Perlt, P. Ray, A. Hansen, F. Malberg, S. Grimme, B. Kirchner, Finding the Best Density Functional Approximation to Describe Interaction Energies and Structures of Ionic Liquids in Molecular Dynamics Studies, J. Chem. Phys. 148 (19) (2018), 193835-1-193835-20.

68. M.G. Del Pópolo, R.M. Lynden-Bell, J. Kohanoff, Ab Initio Molecular Dynamics Simulation of a Room Temperature Ionic Liquid, J. Phys. Chem. B 109 (12) (2005) 5895–5902.

69. P.E. Blöchl, Electrostatic Decoupling of Periodic Images of Plane-Wave-Expanded Densities and Derived Atomic Point Charges, J. Chem. Phys. 103 (17) (1995) 7422–7428.

70. J. Schmidt, C. Krekeler, F. Dommert, Y. Zhao, R. Berger, L.D. Site, C. Holm, Ionic Charge Reduction and Atomic Partial Charges From First-Principles Calculations of 1,3-Dimethylimidazolium Chloride, J. Phys. Chem. B 114 (18) (2010) 6150–6155.

71. C. Krekeler, F. Dommert, J. Schmidt, Y.Y. Zhao, C. Holm, R. Berger, L. Delle Site, Electrostatic Properties of Liquid 1,3-Dimethylimidazolium Chloride: Role of Local Polarization and Effect of the Bulk, Phys. Chem. Chem. Phys. 12 (8) (2010) 1817–1821.

72. F. Dommert, J. Schmidt, C. Krekeler, Y.Y. Zhao, R. Berger, L.D. Site, C. Holm, Towards Multiscale Modeling of Ionic Liquids: From Electronic Structure to Bulk Properties, J. Mol. Liq. 152 (1–3) (2010) 2–8.

73. H. Weber, B. Kirchner, Complex Structural and Dynamical Interplay of Cyano-Based Ionic Liquids, J. Phys. Chem. B 120 (9) (2016) 2471–2483.

74. A.S. Pensado, M. Brehm, J. Thar, A.P. Seitsonen, B. Kirchner, Effect of Dispersion on the Structure and Dynamics of the Ionic Liquid 1-Ethyl-3-methylimidazolium Thiocyanate, ChemPhysChem 13 (7) (2012) 1845–1853.

75. D.S. Firaha, M. Thomas, O. Hollóczki, M. Korth, B. Kirchner, Can Dispersion Corrections Annihilate the Dispersion-Driven Nano-Aggregation of Non-Polar Groups? An Ab Initio Molecular Dynamics Study of Ionic Liquid Systems, J. Chem. Phys. 145 (20) (2016), 204502-1-204502-14.

76. B.L. Bhargava, S. Balasubramanian, Intermolecular Structure and Dynamics in an Ionic Liquid: A Car-Parrinello Molecular Dynamics Simulation Study of 1,3-Dimethylimidazolium Chloride, Chem. Phys. Lett. 417 (4–6) (2006) 486–491.

77. B.L. Bhargava, S. Balasubramanian, Insights Into the Structure and Dynamics of a Room-Temperature Ionic Liquid: Ab Initio Molecular Dynamics Simulation Studies of 1-n-Butyl-3-methylimidazolium Hexafluorophosphate ([bmim][PF 6]) and the [bmim][PF_6]-CO_2 Mixture, J. Phys. Chem. B 111 (17) (2007) 4477–4487.

78. O. Hollóczki, Z. Kelemen, L. Könczöl, D. Szieberth, L. Nyulászi, A. Stark, B. Kirchner, Significant Cation Effects in Carbon Dioxide-Ionic Liquid Systems, ChemPhysChem 14 (2) (2013) 315–320.

79. D.S. Firaha, M. Kavalchuk, B. Kirchner, SO_2 Solvation in the 1-Ethyl-3-methylimidazolium Thiocyanate Ionic Liquid by Incorporation Into the Extended Cation-Anion Network, J. Solut. Chem. 44 (3–4) (2015) 838–849.

80. F. Tang, T. Ohto, T. Hasegawa, M. Bonn, Y. Nagata, π^+-π^+ Stacking of Imidazolium Cations Enhances Molecular Layering of Room Temperature Ionic Liquids at Their Interfaces, Phys. Chem. Chem. Phys. 19 (4) (2017) 2850–2856.

81. Y.L. Wang, A. Laaksonen, M.D. Fayer, Hydrogen Bonding Versus π-π Stacking Interactions in Imidazolium-Oxalatoborate Ionic Liquid, J. Phys. Chem. B 121 (29) (2017) 7173–7179.

82. M. Brehm, D. Sebastiani, Simulating Structure and Dynamics in Small Droplets of 1-Ethyl-3-methylimidazolium Acetate, J. Chem. Phys. 148 (19) (2018), 193802-1-193802-15.

83. M. Campetella, A. Le Donne, M. Daniele, L. Gontrani, S. Lupi, E. Bodo, F. Leonelli, Hydrogen Bonding Features in Cholinium-Based Protic Ionic Liquids From Molecular Dynamics Simulations, J. Phys. Chem. B 122 (9) (2018) 2635–2645.

84. M. Campetella, E. Bodo, M. Montagna, S. De Santis, L. Gontrani, Theoretical Study of Ionic Liquids Based on the Cholinium Cation. Ab Initio Simulations of Their Condensed Phases, J. Chem. Phys. 144 (10) (2016), 104504-1-104504-7.

85. M. Campetella, S. De Santis, R. Caminiti, P. Ballirano, C. Sadun, L. Tanzi, L. Gontrani, Is a Medium-Range Order Pre-Peak Possible for Ionic Liquids Without an Aliphatic Chain?, RSC Adv. 5 (63) (2015) 50938–50941.

86. L. Tanzi, F. Ramondo, R. Caminiti, M. Campetella, A. Di Luca, L. Gontrani, Structural Studies on Choline-Carboxylate Bio-Ionic Liquids by X-ray Scattering and Molecular Dynamics, J. Chem. Phys. 143 (11) (2015), 114506-1-114506-10.

87. L. Gontrani, F. Leonelli, M. Campetella, An X-ray and Computational Study of Liquid Pentylammonium Nitrate, Chem. Phys. Lett. 687 (2017) 38–43.

88. Y. Ando, Y. Kawamura, T. Ikeshoji, M. Otani, Electrochemical Reduction of an Anion for Ionic-Liquid Molecules on a Lithium Electrode Studied by First-Principles Calculations, Chem. Phys. Lett. 612 (2014) 240–244.

89. A. Budi, A. Basile, G. Opletal, A.F. Hollenkamp, A.S. Best, R.J. Rees, A.I. Bhatt, A.P. O'Mullane, S.P. Russo, Study of the Initial Stage of Solid Electrolyte Interphase Formation Upon Chemical Reaction of Lithium Metal and n-Methyl-n-propyl-pyrrolidinium-bis(fluorosulfonyl)imide, J. Phys. Chem. C 116 (37) (2012) 19789–19797.

90. H. Yildirim, J.B. Haskins, C.W. Bauschlicher Jr., J.W. Lawson, Decomposition of Ionic Liquids at Lithium Interfaces. 1. Ab Initio Molecular Dynamics Simulations, J. Phys. Chem. C 121 (51) (2017) 28214–28234.

91. M. Brüssel, M. Brehm, A.S. Pensado, F. Malberg, M. Ramzan, A. Stark, B. Kirchner, On the Ideality of Binary Mixtures of Ionic Liquids, Phys. Chem. Chem. Phys. 14 (38) (2012) 13204–13215.

92. R. Macchieraldo, L. Esser, R. Elfgen, P. Voepel, S. Zahn, B.M. Smarsly, B. Kirchner, Hydrophilic Ionic Liquid Mixtures of Weakly and Strongly Coordinating Anions With and Without Water, ACS Omega 3 (8) (2018) 8567–8582.

93. M.H. Ghatee, A.R. Zolghadr, Local Depolarization in Hydrophobic and Hydrophilic Ionic Liquids/Water Mixtures: Car-Parrinello and Classical Molecular Dynamics Simulation, J. Phys. Chem. C 117 (5) (2013) 2066–2077.

94. S. Zahn, K. Wendler, L. Delle Site, B. Kirchner, Depolarization of Water in Protic Ionic Liquids, Phys. Chem. Chem. Phys. 13 (33) (2011) 15083–15093.

95. M.R. Eliseo, K.J. Shan, J.E. Maginn, Monte Carlo Simulations of Water Solubility in Ionic Liquids: A Force Field Assessment, Fluid Phase Equilibria 407 (2016) 117–125.

96. J.L. Anderson, J.K. Dixon, J.F. Brennecke, Solubility of CO_2, CH_4, C_2H_6, C_2H_4, O_2, and N_2 in 1-Hexyl-3-methylpyridinium Bis(trifluoromethylsulfonyl)imide: Comparison to Other Ionic Liquids, Acc. Chem. Res. 40 (11) (2007) 1208–1216.

97. M.J. Muldoon, S.N.V.K. Aki, J.L. Anderson, J.K. Dixon, J.F. Brennecke, Improving Carbon Dioxide Solubility in Ionic Liquids, J. Phys. Chem. B 111 (30) (2007) 9001–9009, https://doi.org/10.1021/jp071897q.

98. E. Rezabal, T. Schäfer, Ionic Liquids as Solvents of Polar and Non-Polar Solutes: Affinity and Coordination, Phys. Chem. Chem. Phys. 17 (22) (2015) 14588–14597.

99. B.L. Bhargava, M. Saharay, S. Balasubramanian, Ab initio Studies on [bmim][PF_6]-CO_2 Mixture and CO_2 Clusters, Bull. Mater. Sci. 31 (3) (2008) 327–334.

100. L. Gontrani, E. Scarpellini, R. Caminiti, M. Campetella, Bio Ionic Liquids and Water Mixtures: A Structural Study, RSC Adv. 7 (31) (2017) 19338–19344.

101. Y. Zhang, C. Shi, J.F. Brennecke, E.J. Maginn, Refined Method for Predicting Electrochemical Windows of Ionic Liquids and Experimental Validation Studies, J. Phys. Chem. B 118 (23) (2014) 6250–6255.

102. M. Tuckerman, K. Laasonen, M. Sprik, M. Parrinello, Ab Initio Molecular Dynamics Simulation of the Solvation and Transport of Hydronium and Hydroxyl Ions in Water, J. Chem. Phys. 103 (1) (1995) 150–161.

103. N. Agmon, The Grotthuss Mechanism, Chem. Phys. Lett. 244 (5–6) (1995) 456–462.

104. J.G. McDaniel, A. Yethiraj, Grotthuss Transport of Iodide in EMIM/I_3 Ionic Crystal, J. Phys. Chem. B 122 (1) (2017) 250–257.

105. J. Ingenmey, S. Gehrke, B. Kirchner, How to Harvest Grotthuss Diffusion in Protic Ionic Liquid Electrolyte Systems, ChemSusChem 11 (2018) 1900–1910.

106. M. Campetella, M. Montagna, L. Gontrani, E. Scarpellini, E. Bodo, Unexpected Proton Mobility in the Bulk Phase of Cholinium-Based Ionic Liquids: New Insights From Theoretical Calculations, Phys. Chem. Chem. Phys. 19 (19) (2017) 11869–11880.

Keywords: Ionic liquids; Electronic properties; Polarization; Ab initio molecular dynamics; CPMD; First-principles molecular dynamics